doi:10.1093/brain/aws010 Brain 2012: 135; 853–868 | 853

BRAIN
A JOURNAL OF NEUROLOGY

Correlates of spreading depolarization in human scalp electroencephalography

Christoph Drenckhahn,[1,2] Maren K. L. Winkler,[1] Sebastian Major,[1,2,3] Michael Scheel,[4] Eun-Jeung Kang,[1,3] Alexandra Pinczolits,[1,5] Cristian Grozea,[6] Jed A. Hartings,[7] Johannes Woitzik[1,5] and Jens P. Dreier[1,2,3] for the COSBID study group

1 Centre for Stroke Research Berlin, Charité University Medicine Berlin, 10117 Berlin, Germany
2 Department of Neurology, Charité University Medicine Berlin, 10117 Berlin, Germany
3 Department of Experimental Neurology, Charité University Medicine Berlin, 10117 Berlin, Germany
4 Department of Neuroradiology, Charité University Medicine Berlin, 10117 Berlin, Germany
5 Department of Neurosurgery, Charité University Medicine Berlin, 13353 Berlin, Germany
6 Fraunhofer-Institut für Rechnerarchitektur und Softwaretechnik, FIRST, 12489 Berlin, Germany
7 Department of Neurosurgery, University of Cincinnati, Cincinnati 45219, OH, USA

Correspondence to: Jens P. Dreier,
Centre for Stroke Research,
Campus Charité Mitte,
Charité University Medicine Berlin,
Charitéplatz 1, 10117 Berlin,
Germany
E-mail: jens.dreier@charite.de

It has been known for decades that suppression of spontaneous scalp electroencephalographic activity occurs during ischaemia. Trend analysis for such suppression was found useful for intraoperative monitoring during carotid endarterectomy, or as a screening tool to detect delayed cerebral ischaemia after aneurismal subarachnoid haemorrhage. Nevertheless, pathogenesis of such suppression of activity has remained unclear. In five patients with aneurismal subarachnoid haemorrhage and four patients with decompressive hemicraniectomy after malignant hemispheric stroke due to middle cerebral artery occlusion, we here performed simultaneously full-band direct and alternating current electroencephalography at the scalp and direct and alternating current electrocorticography at the cortical surface. After subarachnoid haemorrhage, 275 slow potential changes, identifying spreading depolarizations, were recorded electrocorticographically over 694 h. Visual inspection of time-compressed scalp electroencephalography identified 193 (70.2%) slow potential changes [amplitude: −272 (−174, −375) μV (median quartiles), duration: 5.4 (4.0, 7.1) min, electrocorticography–electroencephalography delay: 1.8 (0.8, 3.5) min]. Intervals between successive spreading depolarizations were significantly shorter for depolarizations with electroencephalographically identified slow potential change [33.0 (27.0, 76.5) versus 53.0 (28.0, 130.5) min, $P = 0.009$]. Electroencephalography was thus more likely to display slow potential changes of clustered than isolated spreading depolarizations. In contrast to electrocorticography, no spread of electroencephalographic slow potential changes was seen, presumably due to superposition of volume-conducted electroencephalographic signals from widespread cortical generators. In two of five patients with subarachnoid haemorrhage, serial magnetic resonance imaging revealed large delayed infarcts at the recording site, while electrocorticography showed clusters of spreading depolarizations with persistent depression of spontaneous activity. Alternating current electroencephalography similarly displayed persistent depression of spontaneous activity, and direct current electroencephalography slow potential changes riding on a shallow negative ultraslow potential. Isolated spreading depolarizations with depression of both spontaneous electrocorticographic and electroencephalographic activity displayed significantly longer intervals between successive spreading depolarizations than isolated depolarizations with only depression of electrocorticographic activity [44.0 (28.0,

Received October 15, 2011. Revised November 23, 2011. Accepted November 23, 2011

132.0) min, *n* = 96, versus 30.0 (26.5, 51.5) min, *n* = 109, *P* = 0.001]. This suggests fusion of electroencephalographic depression periods at high depolarization frequency. No propagation of electroencephalographic depression was seen between scalp electrodes. Durations/magnitudes of isolated electroencephalographic and corresponding electrocorticographic depression periods correlated significantly. Fewer spreading depolarizations were recorded in patients with malignant hemispheric stroke but characteristics were similar to those after subarachnoid haemorrhage. In conclusion, spreading depolarizations and depressions of spontaneous activity display correlates in time-compressed human scalp direct and alternating current electroencephalography that may serve for their non-invasive detection.

Keywords: subarachnoid haemorrhage; spreading depression; delayed cerebral ischaemia; electroencephalography; ischaemic stroke

Abbreviations: AC = alternating current; COSBID = Co-Operative Studies on Brain Injury Depolarizations; DC = direct current; MHS = malignant hemispheric stroke; SAH = subarachnoid haemorrhage

Introduction

In the last decades, hundreds of Phase II and III clinical trials on presumed neuroprotective agents for stroke have failed (see Washington University Internet Stroke Centre, www.strokecenter.org). Therefore, a new road map for neuroprotection has been proposed including better proof of efficacy of neuroprotectants in animal models and efficacy in novel clinical proof of concept studies (Donnan, 2008). In animal experiments, neuroprotectants have been found to be most effective either when given within minutes after the onset of acute neuronal injury or when they have been pre-administered. Moreover, recent experimental evidence suggests that phases of acute injury and repair may require opposing neuroprotective strategies (Lo, 2008). It would thus be promising to develop clinical proof of concept studies where a biomarker can distinguish between phases of acute injury and repair to guide phase-specific treatment allocation of neuroprotectants. Moreover, the biomarker ought to allow a read-out of the neuroprotectant's effect on the parenchyma. Ideally, such a biomarker should reflect neuronal injury in real-time and should be measurable non-invasively.

Spreading depolarization is the mechanism of the abruptly developing cytotoxic oedema in cerebral grey matter (Klatzo, 1987; Dreier, 2011). Spreading depolarization occurs when neuronal cation efflux by the ATP-dependent sodium pumps locally fails to compensate for cation influx of sodium and calcium (Somjen, 2001). The ion fluxes result in a net gain of solutes by the neurons accompanied by water influx. Specifically, spreading depolarization is characterized as a wave of massive ion translocation between intra- and extracellular space, near-complete sustained neuronal depolarization, glial depolarization and neuron swelling. Spreading depolarization is observed as an abrupt, large, negative slow potential change as measured in the low-frequency or direct current (DC) range of the electrocorticogram (Canals *et al.*, 2005; Oliveira-Ferreira *et al.*, 2010; Hartings *et al.*, 2011*b*). In the high-frequency or alternating current (AC) range of the electrocorticography, spreading depolarization causes silencing of spontaneous activity (spreading depression).

Spreading depolarization is induced by energy depletion as well as other stimuli such as chemicals, neurotransmitters and mechanical damage. Spreading depolarization may be followed by either recovery, dependent on sufficient recruitment of sodium pump activity (LaManna and Rosenthal, 1975), or neuronal death (Takano *et al.*, 2007; Risher *et al.*, 2010; Dreier, 2011). Progressive injury and cell death are manifested in a negative ultraslow DC potential, which is possibly of glial and neuronal origin (Herreras and Somjen, 1993; Somjen, 2001; Oliveira-Ferreira *et al.*, 2010). Hence, real-time detection of infarction can be achieved using electrodes on the brain surface over the newly developing infarct through measurement of the large negative ultraslow DC potential on which one or more slow potential changes/spreading depolarizations are riding (Oliveira-Ferreira *et al.*, 2010). However, spreading depolarizations typically propagate away from or circle around the infarcted tissue at a speed of ~3 mm/min (Nakamura *et al.*, 2010). Even remote from the actual infarct, recording electrodes may therefore identify occurrence of a new infarct when a cluster of recurrent, short-lasting spreading depolarizations is recorded (Dreier *et al.*, 2006; Dohmen *et al.*, 2008). Spreading depolarizations of such a cluster ride on a shallow negative ultraslow potential in the ischaemic penumbra (current sink), whereas they ride on a shallow positive potential in the normally perfused surrounding tissue (current source) (Oliveira-Ferreira *et al.*, 2010). Between recurrent spreading depolarizations, normally perfused tissue immediately around the penumbra shows persistent depression of spontaneous activity in similar fashion to the penumbra, whereas repeated cycles of spreading depression of spontaneous activity followed by recovery are observed further away (Oliveira-Ferreira *et al.*, 2010; Hartings *et al.*, 2011*b*). Whether and how zonal gradients of the slow potentials along laminar profiles across the cortex reflect such interregional electrophysiological differences in and around ischaemic zones has not been studied sufficiently while current sources and sinks are well established for epileptic seizure activity and spreading depolarization in otherwise healthy tissue (Wadman *et al.*, 1992).

Currently, clinical monitoring of spreading depolarizations is limited to patients who require neurosurgical interventions that allow for placement of a subdural electrode strip such as surgical aneurysm ligation after subarachnoid haemorrhage (SAH), placement of extraventricular drainage, decompressive hemicraniectomy or evacuation of a haematoma (Strong *et al.*, 2002; Dreier *et al.*, 2006; Dohmen *et al.*, 2008). Thus, spreading depolarizations have been recorded in abundance in individuals with aneurismal SAH, delayed ischaemic stroke after aneurismal SAH, malignant

hemispheric stroke (MHS), spontaneous intracerebral haemorrhage or traumatic brain injury (Strong *et al.*, 2002; Dreier *et al.*, 2006, 2009; Fabricius *et al.*, 2006; Dohmen *et al.*, 2008; Hartings *et al.*, 2011*b*). Nevertheless, the monitoring of spreading depolarizations could be extended to other patient populations if non-invasive technology allowed their reliable detection. Here, we investigated whether ultraslow DC potential, slow potential change and/or depression of spontaneous activity can be recorded using scalp DC/AC-EEG while occurrence of those signals was validated at the brain surface using invasive near-DC/AC-electrocorticography or DC/AC-electrocorticography.

Patients and methods

Patient recruitment

Five patients with aneurismal SAH and four patients with MHS were recruited at two centres of the Charité University Medicine Berlin participating in the Co-Operative Studies on Brain Injury Depolarizations (COSBID) [Campus Virchow Klinikum ($n = 5$) and Campus Benjamin Franklin ($n = 4$)]. Inclusion criteria were age $\geqslant$18 years and the clinical decision for either craniotomy to perform surgical ligation of an aneurysm, evacuation of a haematoma and/or decompression, or for an extended burr hole to place a ventricular drain or oxygen sensor. Patients with fixed, dilated pupils were excluded. Research protocols were approved by the institutional review board and surrogate informed consent was obtained for all patients. All research was conducted in accordance with the Declaration of Helsinki. Aneurismal SAH and MHS were diagnosed by the assessment of CT and CT angiography scans. In three patients with aneurismal SAH, additional digital subtraction angiography was performed initially.

At the conclusion of surgery, a single, linear, six-contact (platinum) recording strip (Wyler, 5 mm diameter; Ad-Tech Medical) was placed on the surface of the cortex for subsequent electrocorticography recordings (Strong *et al.*, 2002; Dreier *et al.*, 2006; Dohmen *et al.*, 2008). After surgery, patients were transferred to the intensive care unit where continuous electrocorticography and EEG recordings were acquired for up to 15 days after aneurismal SAH and up to 8 days after MHS. Thereafter, electrode strips were removed at the bedside by gentle traction. No haemorrhagic or infectious complications of the electrode strip were encountered. Clinical outcome was assessed using the modified Rankin Scale on Day 15 after aneurismal SAH and on Day 8 after MHS.

Throughout recordings, patients were ventilated and pharmacologically immobilized as required. Sedation was mostly maintained with propofol or midazolam, and analgesia was provided with fentanyl. Intracranial pressure was monitored, if clinically indicated, by a ventricular drainage catheter or an intraparenchymal intracranial pressure transducer (Codman). Glasgow Coma Score, blood gases, glucose and electrolytes were documented at least every 6 h. A thorough neurological examination was performed at least daily.

Patients with aneurismal subarachnoid haemorrhage

Clinical presentation of aneurismal SAH was classified according to the World Federation of Neurological Surgeons scale. Amount and distribution of subarachnoid blood was graded according to the Fisher scale (Kistler *et al.*, 1983). After diagnosis of aneurismal SAH, surgical and/or endovascular interventions were performed within the next 24 h. Three patients underwent surgical clipping, one endovascular coiling and one was initially coiled followed by clipping due to aneurysm rupture in the course of coiling. The recording strip was positioned on viable, but often oedematous tissue.

A delayed ischaemic neurological deficit was defined as the occurrence of focal neurological impairment (such as hemiparesis, aphasia, apraxia, hemianopia or neglect), or a decrease of at least two Glasgow Coma Scale points [either on the total score or on one of its individual components (eye, motor on either side, verbal)]. Moreover, the diagnosis of a delayed ischaemic neurological deficit required that the neurological deficit was not present immediately after aneurysm occlusion, that it lasted for at least 1 h, could not be attributed to other causes such as hydrocephalus or re-bleeding by means of clinical assessment, CT or MRI of the brain, and appropriate laboratory studies, and did not occur earlier than 72 h after the initial haemorrhage (Vergouwen *et al.*, 2010). Serial MRI scans were performed postoperatively, at the time of clinical deterioration and after the monitoring period to screen for delayed infarcts. Admission and follow-up neuroimages were independently evaluated by a study neuroradiologist (M.S.), blinded to the electrocorticography data, for the presence of focal or global cerebral oedema, the Fisher grade, the presence and degree of hydrocephalus, the presence of infarction, intracerebral or subdural haematoma.

Criteria for proximal vasospasm after aneurismal SAH were defined using digital subtraction angiography as $>$30% narrowing of the arterial luminal diameter in one of the following arterial segments: A1, A2, M1, M2 and C1–C2. Magnification errors were corrected by comparing extradural segments of the internal carotid artery (C4–C5). Using transcranial Doppler sonography, significant vasospasm was defined by a mean velocity $\geqslant$200 cm/s in at least one middle cerebral artery (Vora *et al.*, 1999). Vasospasm was excluded if the middle cerebral artery mean velocities remained $<$120 cm/s throughout the observation period.

Patients with delayed cerebral ischaemia were treated with haemodynamic therapy (hypertension, hypervolaemia) (van Gijn and Rinkel, 2001). Oral nimodipine was given prophylactically in all patients.

Patients with malignant hemispheric stroke

Clinical presentation of MHS was classified according to the National Institute of Health Stroke Scale. All patients with MHS suffered from $\geqslant$2/3 infarction of the middle cerebral artery territory. Hemicraniectomy was initiated following similar in- and exclusion criteria as recently published for DESTINY II (Juttler *et al.*, 2011), but inclusion criterion for age was $\geqslant$18 years. In patients with MHS, the electrode strip was implanted over presumed viable peri-infarct tissue of the anterior cerebral artery. The electrode was advanced under the bone rim to ensure proper fixation so that the strip was placed tangentially in relation to the border of infarction. The lead wire of the strip was externalized through a burr hole in the skull (if the bone flap was replaced) and tunnelled beneath the scalp to exit 2–3 cm from the craniotomy margin.

Near-DC/AC- and DC/AC-electrocorticography recordings at the cortical surface

Two ipsilateral, subdermal platinum needle electrodes (SpesMedica) served as reference and ground for the invasive, subdural recordings.

Near-DC/AC-electrocorticography signals were recorded by a GT205 amplifier (bandpass: 0.01–45 Hz, sampling rate: 200 Hz) connected to a Powerlab 16/SP analogue/digital converter (ADInstruments). In some patients, electrocorticography was measured in parallel using a BrainAmp amplifier in order to record DC in addition to near-DC potential components (bandpass: 0–1000 Hz, sampling rate: 2500 Hz, BrainAmp MR plus, Brain Products). Subdural electrodes were connected in sequential bipolar fashion as well as in unipolar fashion, each referenced to the ipsilateral subdermal platinum electrode. Data were recorded and reviewed with the use of LabChart 7 software (ADInstruments) and BrainVision Recorder 1.05 software (Brain Products), respectively.

Scalp DC/AC-EEG recordings

In order to monitor the full-band DC/AC–EEG (bandpass: 0–1000 Hz, sampling rate: 2500 Hz), sintered Ag/AgCl electrodes (EasyCap) were connected to a BrainAmp amplifier. The number of recording electrodes varied from 8 to 13 depending on the scalp area shaved for the neurosurgical procedure and the localization of exit points from the skull for invasive probes such as the external ventricular drain. Ipsilateral to the electrocorticography strip, 6–8 scalp electrodes were placed covering the frontal, parietal and temporal brain regions; 2–5 electrodes were placed contralaterally. Electrodes were positioned in accordance to the international 10–20 electrode system (Klem *et al.*, 1999). The reference electrode was placed on the mastoid ipsilateral to the electrocorticography recording strip. An electrode in the frontal midline served as ground. The electrodes were attached with Collodion adhesive (Mavidon). Abrasive electrode gel (Abralyt 2000, EasyCap) and conductive electrode cream (Synapse, Med-Tek) were applied to set the electrode impedance to $<5\,k\Omega$ and to assure long-term stability of the signal with minimal DC potential drifts. The EEG signal was recorded using BrainVision Recorder 1.05 software.

Data processing and analysis

Spreading depolarizations were identified in the subdural recordings by (i) the simultaneous occurrence of a slow potential change in the DC or near-DC frequency range (<0.05 Hz), and depression of spontaneous activity in the AC frequency range ($\sim$0.5–45 Hz) in individual channels; and (ii) the sequential occurrence of slow potential change and depression on adjacent channels, evidencing the propagation of spreading depolarization across the cortex as described previously (Fabricius *et al.*, 2006). Depression durations were scored beginning at the initial decrease in the integral (60 s decay time constant) of the power of the AC-electrocorticography and ending at the start of the recovery phase as described previously (Dreier *et al.*, 2006) (Fig. 1A). The integral of the power is based on a method of computing time integrals with a reset type that resets the integral periodically after a given time, in the manner of decay such as that found in a 'leaky' analogue integrator. This mathematical procedure provides a smoothed curve easing visual assessment of changes in AC-electrocorticography power. The method has become standard to score depression periods of spreading depolarizations (Dreier *et al.*, 2006; Dohmen *et al.*, 2008; Hartings *et al.*, 2011*b*) and is useful in the screening for ictal epileptic activity (Fabricius *et al.*, 2008; Dreier *et al.*, 2012). In this article, depression periods were scored in each of the five bipolar electrocorticography channels (electrode 1–2, 2–3, 3–4, 4–5 and 5–6) to determine longest and shortest depression period of each spreading depolarization.

Slow potential changes also occurred in some cases when the AC-electrocorticography band was flat, or isoelectric, and therefore lacked depression periods. Baseline isoelectricity may result from non-spreading depression of activity as described previously (Leão, 1947; Dreier, 2011), or from a persistent depression period of a preceding spreading depolarization (Dreier *et al.*, 2006; Fabricius *et al.*, 2006; Dohmen *et al.*, 2008; Oliveira-Ferreira *et al.*, 2010; Hartings *et al.*, 2011*b*). Slow potential changes occurring in a stereotyped and propagating manner in isoelectric tissue are termed 'silent' spreading depolarizations in the present paper. In a previous paper, the term 'isoelectric' spreading depolarization was used (Hartings *et al.*, 2011*b*). Both terms refer to the same phenomenon. The term 'isoelectric' spreading depolarization does not imply that the slow potential change remains undetected by the electrocorticography recording.

Apparent propagation velocities were calculated from the DC- or near-DC-electrocorticography signals as the 10-mm separation between subdural electrodes divided by the time interval between the onsets of the slow potential change at adjacent electrodes.

Because of the substantial spatial distance between EEG electrodes at the scalp and subdural electrocorticography electrodes at the brain surface, EEG depressions were accepted as co-registrations in a range of ±15 min around time points of spreading depolarization appearance in the subdural electrodes. Such spatial distance may lead to a substantial time displacement of the co-registration. Although a 30-min window was thus considered for analysis around the electrocorticography starting point of spreading depolarization, the actual delay observed was in general much lower, with a median <6 min (see below).

Durations of EEG depressions were quantified in a similar fashion to electrocorticography depressions beginning at the initial decrease in the integral (60 s decay time constant) of the power of the AC-EEG and ending at the start of the recovery phase (Fig. 1A). We arbitrarily considered EEG depressions as significant if a deviation of the integral of power from the baseline (average of 10 min immediately preceding the drop in integral of power) to a level of $\leqslant85\%$ was detected. Amplitudes of the slow potential changes were measured in the DC-EEG from the baseline to the peak negativity (Fig. 1A). Electrocorticography data were analysed by M.W. blinded to the clinical courses and radiological findings. Spreading depolarization time points were then given to C.D. who analysed the EEG data blinded to the durations of the electrocorticography depression periods, the clinical courses and radiological findings. Thereafter, J.D. performed the statistical comparisons between electrocorticography and EEG data provided by M.W. and C.D. blinded to the clinical courses and radiological findings.

Data are given as median (1st, 3rd quartile). Statistical analysis was performed using Mann–Whitney Rank Sum Tests and Spearman's Rank Order Correlations as indicated in the text. $P < 0.05$ was considered statistically significant.

Results

Slow potential changes in scalp and cortical surface recordings of patients with aneurismal subarachnoid haemorrhage

Demographic details are given in Table 1. During 1255.2 h of near-DC/AC-electrocorticography recording time from the cortical

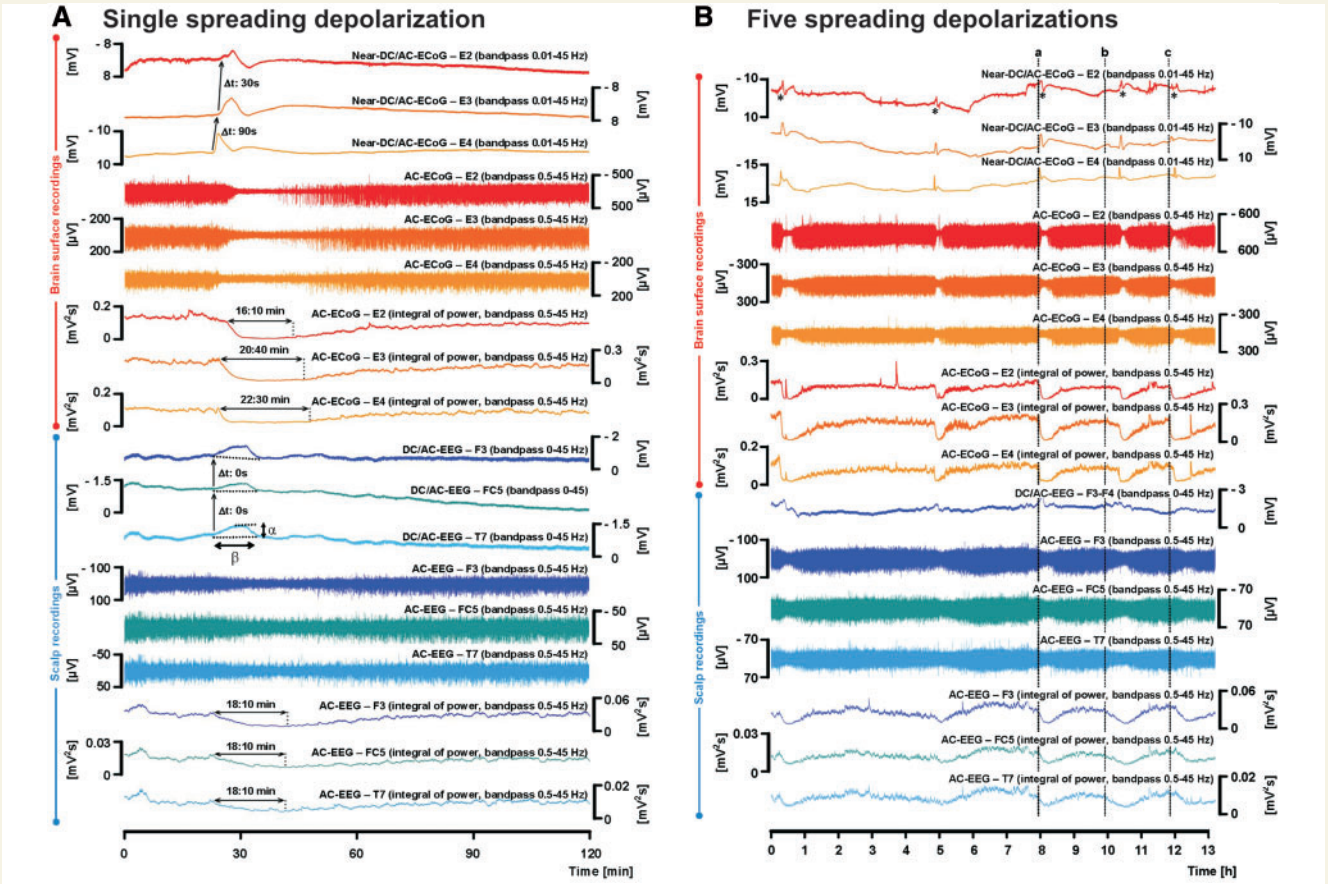

Figure 1 (**A**) Simultaneous recording of spreading depolarization with spreading depression of spontaneous activity in a patient with aneurismal SAH (Case 1 in Table 1) using electrodes at the cortical surface (electrocorticography; ECoG) and scalp EEG. Recordings were performed on Day 5 after aneurismal SAH. Traces 1–9 show the electrocorticography at electrodes E2, E3 and E4 (red, orange and yellow) (subdural electrode strip), whereas traces 10–18 give the EEG at the ipsilateral scalp electrodes F3, FC5 and T7 (dark blue, green and light blue) (international 10–20 electrode system). Traces 1–3 (near-DC/AC-electrocorticography) and traces 10–12 (DC/AC-EEG) display the slow potential change that identifies spreading depolarization. Traces 4–6 (AC-electrocorticography) and 13–15 (AC-EEG) show the associated depression of spontaneous activity in the conventional EEG bandwidth >0.5 Hz. The integral of power of the conventional EEG bandwidth is calculated in traces 7–9 (AC-electrocorticography) and 16–18 (AC-EEG). The figure illustrates how the integral of power is used to score the duration of the depression period from the initial decrease to the start of the recovery phase. Note slow potential change propagation from electrode E4 to E3 to E2 in cortical surface recordings of traces 1–3 (arrows). In contrast, no spread of the slow potential change is identified by visual inspection of the scalp EEG measurements in traces 10–12 (arrows). In similar fashion, propagation of the depression of spontaneous activity is only seen between subdural electrodes (traces 4–9) but not between scalp electrodes (traces 13–18). Moreover, the duration of the depression period is similar at the three scalp electrodes in contrast to subdural recordings where the duration of the depression period differs between electrodes. This inter-regional uniformity of the scalp EEG is due to summation of volume conducted scalp EEG signals from generators widely distributed over the whole hemisphere (see text). Amplitudes of the slow potential changes (α) were measured in the DC-EEG from the baseline (β) to the peak negativity as shown in trace 12. (**B**) Series of five spreading depolarizations (marked by asterisk in trace 1) associated with depression of spontaneous activity recorded by electrocorticography and EEG. The recordings are from the same patient and day as those in (**A**) (delay between **A** and **B**: 8 h and 30 min). Traces 1–9 (red, orange and yellow) show the electrocorticography at subdural electrodes E2, E3 and E4 while traces 10–16 (dark blue, green and light blue) give the EEG at the ipsilateral scalp electrodes. Traces 1–3 (near-DC/AC-electrocorticography) and trace 10 (DC/AC-EEG) display the slow potential changes that identify the spreading depolarizations. Traces 4–6 (AC-electrocorticography) and 11–13 (AC-EEG) show the associated depression of spontaneous activity in the conventional EEG bandwidth >0.5 Hz. The integral of power of the conventional EEG bandwidth is calculated in traces 7–9 (AC-electrocorticography) and 14–16 (AC-EEG). Note the recording time of 13.5 h. Also note that the near-DC-electrocorticography recordings of the slow potential changes at the brain surface indicate that the paths of spreading depolarization in the cortex change from third to fourth to fifth spreading depolarization, so the temporal relationships between electrocorticography and EEG vary between the subsequent spreading depolarizations. Thus, the depression of spontaneous activity of the third spreading depolarization starts almost simultaneously in AC-electrocorticography and AC-EEG (marked by broken line a), whereas the depression of the fourth spreading depolarization starts in the AC-EEG prior to the AC-electrocorticography (marked by broken line b) and the depression of the fifth spreading depolarization starts in the AC-electrocorticography prior to the AC-EEG (marked by broken line c). Similar temporal relationships between cortical surface and scalp also apply to the slow potential changes. Varying paths of spreading depolarizations in the cortex thus translate into slightly varying patterns of slow potential changes and depressions in the scalp DC/AC-EEG.

Table 1 Summary of demographic, treatment and spreading depolarization-related data of the patients

No.	Age (years), sex	WFNS grade	Fisher grade	Location of aneurysm	Significant proximal vas-spasm	Delayed CT or MRI proven infarct	Intervention	Location of electrode strip	Start of ECoG monitoring (day after insult)	ECoG recording time (h)	No. of SDs in the ECoG	Start of simultaneous ECoG/EEG monitoring (day after insult)	Simultaneous ECoG/EEG recording time (h)	No. of SDs in the simultaneous ECoG/EEG recordings	mRS on Day 14
SAH															
1	49, F	2	3	PCoA	Yes	Yes	Aneurysm clipping, EVD	Left frontal cortex	0	131.9	38	0	57.5	28	6
2	68, F	4	3	PCoA	Yes	Yes	Aneurysm clipping, EVD	Left frontal cortex	1	258.7	150	1	180.3	53	6
3	48, M	4	3	BA	Yes	No	Aneurysm coiling, EVD	Right frontoparietal cortex	3	269.6	3	3	43.3	3	5
4	63, M	5	3	ACoA	Yes	Yes	Aneurysm coiling and clipping, EVD	Left frontal cortex	0	303.8	16	1	49.8	4	5
5	55, F	4	3	MCA	Yes	Yes	Aneurysm clipping, EVD, hemi-craniectomy	Right frontal cortex	0	291.2	191	1	263.2	187	5

No.	Age (years), sex	Cause of MHS	Side	territory	Intervention	Location of electrode strip	Start of ECoG monitoring (day after insult)	ECoG recording time (h)	No. of SDs in the ECoG	Start of simultaneous ECoG/EEG monitoring (day after insult)	Simultaneous ECoG/EEG recording time (h)	No. of SDs in the simultaneous ECoG/EEG recordings	mRS on Day 8
MHS													
6	71, F	ICA occlusion	Left	MCA + ACA	EVD, hemicraniectomy	Left frontal cortex	1	154.6	1	1	65.5	1	5
7	49, F	MCA occlusion	Left	MCA	EVD, hemicraniectomy	Left frontal cortex	1	62.9	24	1	20.1	0	5
8	70, M	MCA occlusion	Right	MCA	EVD, hemicraniectomy	Right frontal cortex	1	176.3	43	1	138.1	18	5
9	54, M	MCA occlusion	Left	MCA	Lysis, EVD, hemicraniectomy	Left frontal cortex	1	81.8	11	1	44.6	1	5

ACA = anterior cerebral artery; ACoA = anterior communicating artery; BA = basilar artery; ECoG = electrocorticography; EVD = extraventricular drainage; F = female; ICA = internal carotid artery; M = male; MCA = middle cerebral artery; mRS = modified Rankin Scale; PCoA = posterior communicating artery; SD = spreading depolarization; WFNS = World Federation of Neurological Surgeons Scale.

Table 2 Comparison between near-DC/AC-electrocorticography and DC/AC-EEG findings in the five patients with aneurismal SAH

Spreading depolarizations in near-DC/AC-ECoG	Proportion of depression periods with a correlate in the AC-EEG	Proportion of SPCs with an SPC correlate in the DC-EEG
Pattern 1: silent spreading depolarizations characterized by persistent depression of spontaneous activity between SPCs ($n = 36$ spreading depolarizations).	Persistent depression of spontaneous activity between SPCs in 2 of 2 patients.	72.2% (SPCs ride on a negative ultraslow potential in 2 of 2 patients).
Pattern 2: spreading depolarizations with depression of spontaneous activity ($n = 239$ spreading depolarizations).	Depression period of spontaneous activity is detected in 46.8% of these spreading depolarizations (34 spreading depolarizations were excluded from this analysis because of an artefact due to the BrainAmp amplifier).	69.9%
	Intervals between successive spreading depolarizations: 44.0 (28.0, 132.0) versus 30.0 (26.5, 51.5) min, detected versus undetected depression periods ($P = 0.001$).	Intervals between successive spreading depolarizations: 33.0 (27.0, 76.5) versus 53.0 (28.0, 130.5) min, detected versus undetected SPCs ($P = 0.009$).

ECoG = electrocorticography; SPC = slow potential change.

surface, the five patients with aneurismal SAH had a total of 398 spreading depolarizations. For further analysis, 694.0 h of simultaneous subdural near-DC/AC-electrocorticography and scalp DC/AC-EEG recording time was available during which 275 of the 398 spreading depolarizations occurred. Slow potential changes of these 275 spreading depolarizations showed a peak-to-peak amplitude of 1.2 (0.8, 1.8) mV (median, quartiles) in the near-DC-electrocorticography recordings; propagation velocity was 5.7 (2.9, 8.2) mm/min assuming an ideal linear spread along the subdural electrode strip. Slow potential change duration was not determined since slow potential change distortion in near-DC recordings precludes assessment of slow potential change duration (Hartings *et al.*, 2009). Subsequently, visual inspection of scalp DC-EEG recordings identified 193 of 275 slow potential changes (70.2%) as illustrated in Figs 1, 2E, 3, 4E and 5. Of note, the intervals between successive spreading depolarizations were significantly shorter, as measured in near-DC-electrocorticography, for spreading depolarizations which displayed the slow potential change in DC-EEG [33.0 (27.0, 76.5) versus 53.0 (28.0, 130.5) min, $P = 0.009$, $n = 273$, Mann–Whitney Rank Sum Test] (Table 2). In other words, DC-EEG was more likely to detect slow potential changes of clustered than isolated spreading depolarizations. Such slow potential changes of clustered, highly frequent spreading depolarizations are shown in Fig. 3B. This observation may indicate that, statistically, larger areas of cortex are simultaneously depolarized in clustered compared with isolated spreading depolarizations.

Median slow potential change amplitude was −272 (−174, −375) μV (range: −65 to −1090 μV) and median slow potential change duration was 5.4 (4.0, 7.1) min in scalp DC-EEG recordings (Fig. 1A). Delay between slow potential change onsets in brain surface near-DC-electrocorticography and scalp DC-EEG recordings was 1.8 (0.8, 3.5) min. Different from subdural electrodes, no spread of the slow potential change was seen between scalp electrodes (Fig. 1A).

The signature of delayed cerebral ischaemia in scalp and cortical surface recordings

Thirty-six of the 275 spreading depolarizations represented silent, clustered spreading depolarizations in the near-DC/AC-electrocorticography recordings. 'Silent' means that spontaneous activity had already ceased before the onset of spreading depolarization. Such silent spreading depolarizations cannot lead to a further clinical deficit in the neurological function represented in the parenchyma undergoing the depolarization as this function was already lost due to the preceding depression of activity (Dreier, 2011; Oliveira-Ferreira *et al.*, 2012). Nevertheless, such silent spreading depolarizations may determine whether this function will be lost permanently as they may damage the neurons irreversibly (Hossmann, 1994; Dreier *et al.*, 2006; Fabricius *et al.*, 2006; Oliveira-Ferreira *et al.*, 2010; Hartings *et al.*, 2011*a, b*). The persistent depression of spontaneous activity between the silent spreading depolarizations in the AC-electrocorticography was well reflected by the persistent depression of spontaneous activity in the AC-EEG in each case, as illustrated in Fig. 2E. Simultaneously with the silent spreading depolarizations in the near-DC/AC-electrocorticography, DC-EEG displayed slow potential changes riding on a negative ultraslow potential (Fig. 2E).

It has been shown previously that such electrocorticography clusters of recurrent silent spreading depolarizations are associated with delayed ischaemic infarcts after aneurismal SAH (Dreier *et al.*, 2006). Consistently, the cluster of silent spreading depolarizations, demonstrated in Fig. 2E, was associated with a large, new delayed ischaemic infarct in the ipsilateral hemisphere during the recording period, as illustrated in the MRI scans of Fig. 2C1 and C2 compared with those of the preceding MRI shown in Fig. 2B1 and B2. Figure 2A1, A2 and 2D demonstrate localization of subdural recording strip and scalp electrode array, respectively.

In another patient, the subdural DC/AC-electrocorticography was recorded over the infarcting area during infarct evolution in

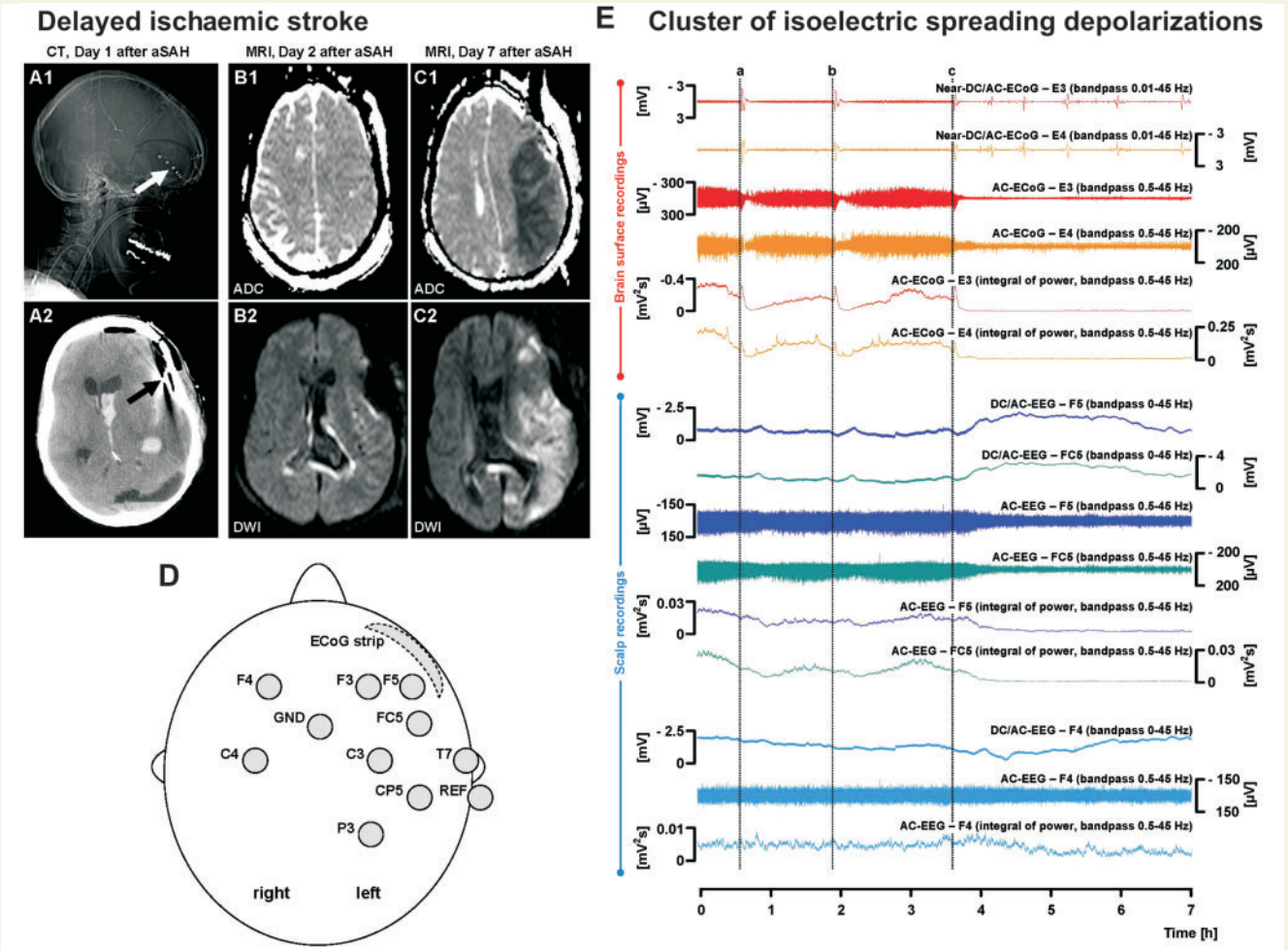

Figure 2 Development of a large delayed ischaemic infarct at the recording area during the monitoring period. (**A1**) The CT scout view shows the orientation of the electrocorticography (EoG) recording strip (marked by white arrow). (**A2**) CT scan showing location of subdural electrode E2 (marked by black arrow). (**B1**) Apparent diffusion coefficient (ADC) map, and (**B2**) diffusion weighted imaging (DWI) of MRI on Day 2 after aneurismal SAH (aSAH). (**C1**) Apparent diffusion coefficient map, and (**C2**) diffusion weighted imaging scan of MRI on Day 7 after aneurismal SAH. Note that the MRI scans of Day 7 display a large new delayed ischaemic infarct in the left middle cerebral artery and posterior cerebral artery territories. (**D**) Scalp electrode array following the 10–20 system, and electrocorticography recording strip. (**E**) Transition from spreading depolarizations associated with depression of spontaneous activity to a cluster of silent spreading depolarizations with persistent depression of activity. The electrocorticography and EEG traces are from the same patient as those in Fig. 1 but only recorded on Day 6 after aneurismal SAH between the two MRIs shown in (**B**) and (**C**). Traces 1–6 give the electrocorticography at electrodes E3 (red) and E4 (orange), and traces 7–12 the EEG at the ipsilateral scalp electrodes F5 (dark blue) and FC5 (green). Traces 13–15 display the EEG at the contralateral scalp electrode F4 (light blue). Traces 1 and 2 (near-DC/AC-electrocorticography) and traces 7 and 8 (DC/AC-EEG) display the slow potential changes that identify the spreading depolarizations. Traces 3 and 4 (AC-electrocorticography) and 9 and 10 (AC-EEG) show the associated depression of spontaneous activity in the conventional EEG bandwidth >0.5 Hz. The integral of power of the conventional EEG bandwidth is calculated in traces 5 and 6 (AC-electrocorticography) and 11 and 12 (AC-EEG). The first two spreading depolarizations during this recording period of 7 h are associated with depression of spontaneous activity followed by recovery (marked by broken lines a and b). The third spreading depolarization (marked by broken line c) initiates the persistent spreading depression of spontaneous activity during which the electrocorticography displays five silent spreading depolarizations ('silent' means that spontaneous activity has already ceased before spreading depolarization onset, see text). Note that the persistent depression of spontaneous AC-electrocorticography activity (traces 3–6) is accompanied by simultaneous depression of spontaneous AC-EEG activity (traces 9–12). Also note the onset of a negative ultraslow potential in scalp electrodes F5 and FC5 (traces 7 and 8) marked by broken line c. In animals, slow potential changes riding on such negative ultraslow potentials are the characteristic signature of neuronal injury (Herreras and Somjen, 1993; Oliveira-Ferreira *et al.*, 2010). Changes at the contralateral electrode F4 are much less pronounced. The mild AC-EEG depression at the contralateral electrode may be caused by the ipsilateral reference at the mastoid. GND = ground; REF = reference.

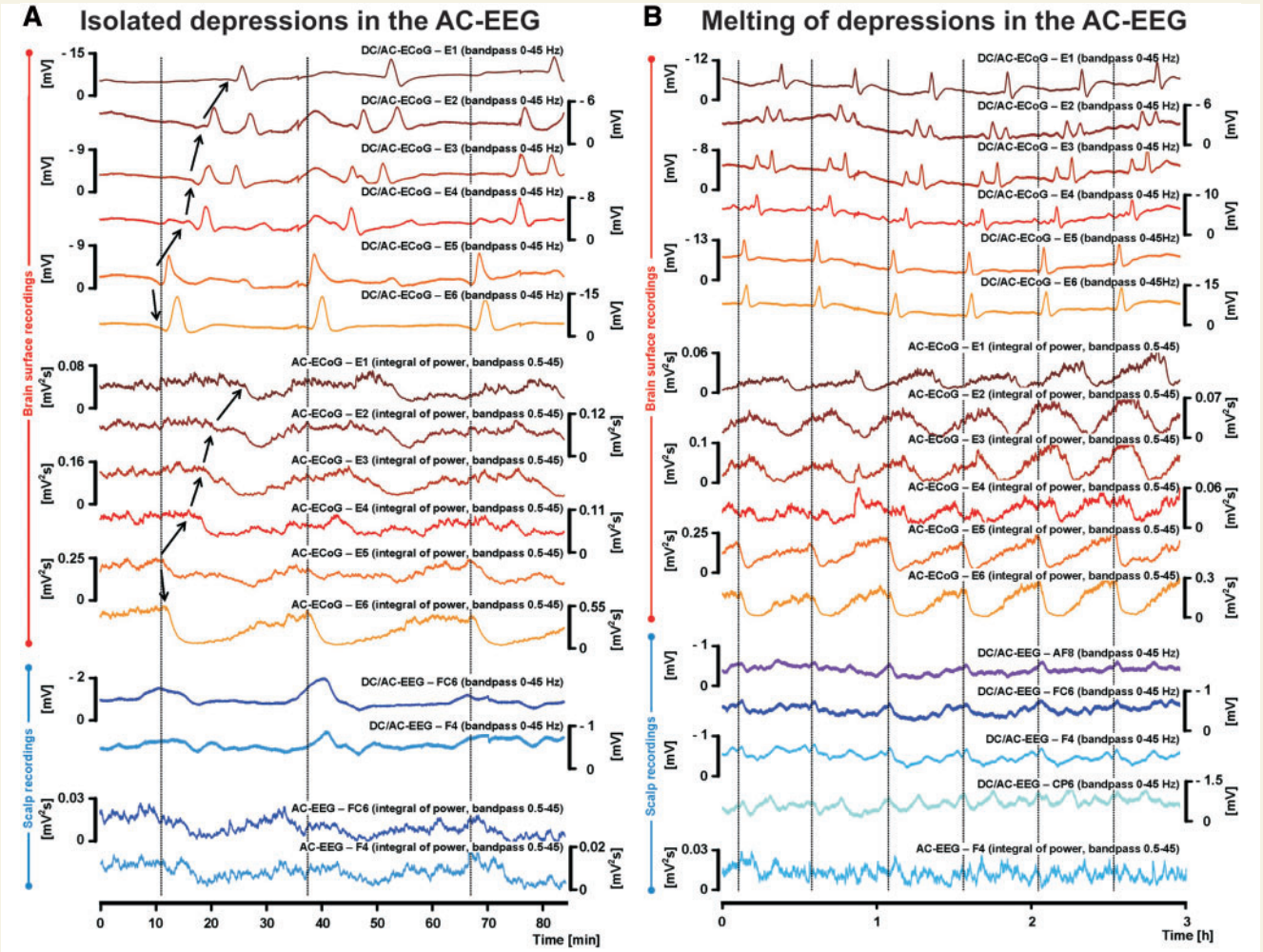

Figure 3 Cluster of repetitive spreading depolarizations in a patient developing a delayed ischaemic infarct remote from the subdural recording strip (Case 5 in Table 1). (**A**) Traces 1–6 display the DC/AC-electrocorticography (ECoG) at subdural electrodes E1–E6. Note the slow potential changes that identify three spreading depolarizations in this episode of 80 min duration (vertical lines). The slow potential changes seem to propagate from electrode E5 to the other electrodes (arrows). Also note large amplitudes of the slow potential changes and slow potential changes with two or even three peaks at electrodes E2 to E5. Such twin peaks could reflect longer depolarizations in deeper layers of the cortex (Herreras and Somjen, 1993). Traces 7–12 give the simultaneous integrals of AC-electrocorticography power demonstrating cycles of spreading depression of spontaneous activity (arrows) followed by recovery. Traces 13 and 14 display the slow potential changes at scalp electrodes FC6 (dark blue) and F4 (light blue) that correspond to the slow potential changes at the cortical surface. The integrals of EEG power in traces 15 (electrode FC6) and 16 (electrode F4) show isolated cycles of depression in spontaneous activity followed by recovery similar to the invasive recordings. In contrast to the subdural recordings, no propagation of slow potential changes and depression periods is observed between scalp electrodes. (**B**) One day later, spreading depolarizations continue to recur at high frequency. Arrangement of traces, electrodes and filter settings is similar to (**A**) but the DC/AC-EEG recordings at scalp electrodes AF8 and CP6 are demonstrated in addition to those at scalp electrodes FC6 and F4 to illustrate variations in scalp slow potential change patterns. Note correspondence between slow potential changes at scalp and cortical surface (vertical lines). It seems that subsequent depression periods are fused at scalp electrode F4 (integral of power in trace 17) although subdural electrodes still show isolated cycles of spreading depression followed by recovery of spontaneous activity at the cortical surface.

addition to the routine near-DC/AC-electrocorticography (Figs 4 and 5). As described previously during infarct evolution in animals (Herreras and Somjen, 1993; Hossmann, 1994; Oliveira-Ferreira *et al.*, 2010), slow potential changes at the cortical surface rode on a characteristic local negative ultraslow injury potential (Fig. 5). DC-EEG recordings simultaneously displayed slow potential changes riding on a shallow negative ultraslow potential at the scalp. Drop in integral of AC-EEG power, indicating persistent depression of spontaneous activity at the scalp, displayed a similar time course as drop in integral of AC-electrocorticography power, indicating persistent depression of spontaneous activity at the brain surface (Fig. 5).

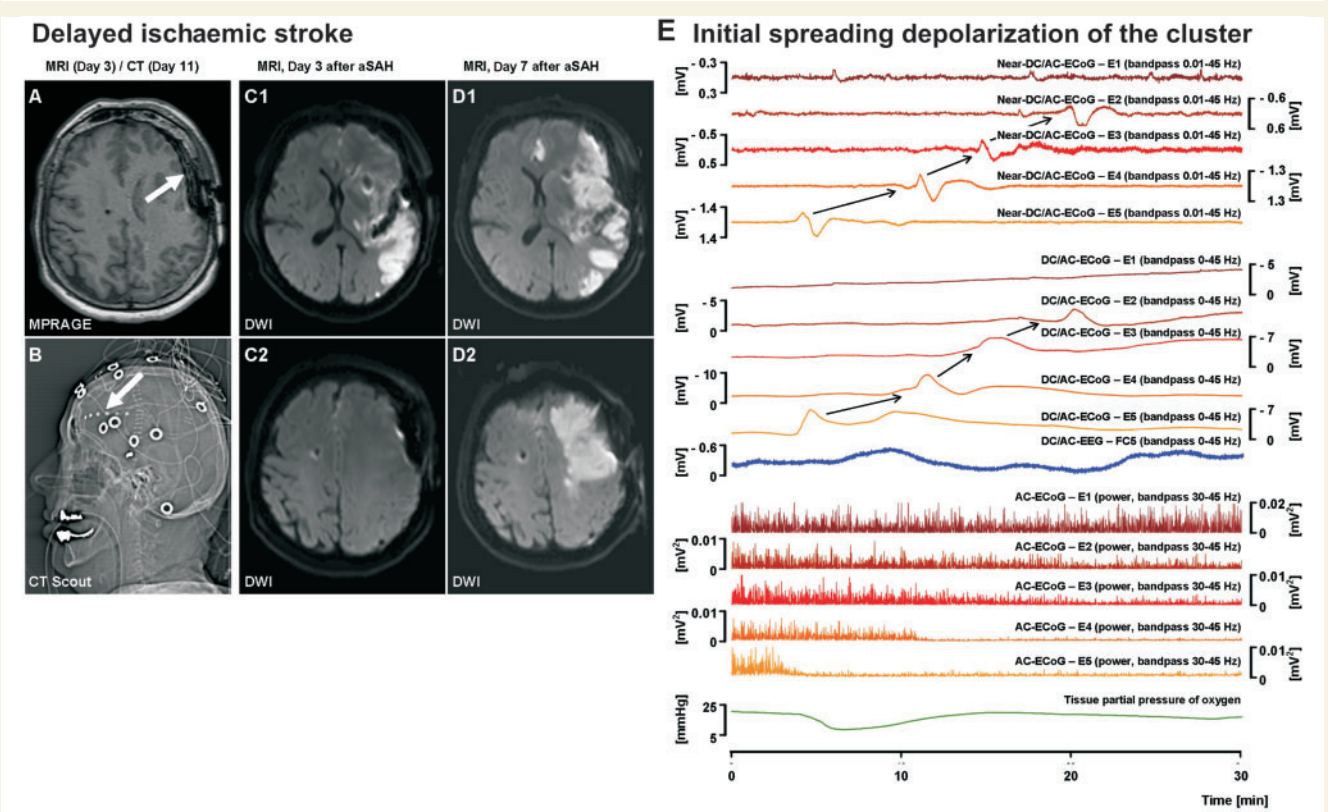

Figure 4 Development of a large delayed ischaemic infarct at the recording area during the monitoring period (Case 2 in Table 1). (**A**) MPRAGE (magnetization prepared rapid gradient echo)-sequence, a T_1-weighted, gradient-echo sequence visualizing the subdural recording strip (marked by white arrow). (**B**) The CT scout view shows the orientation of the electrocorticography (ECoG) recording strip (marked by white arrow). (**C1** and **C2**) Diffusion weighted MRI (DWI) shows an infarct in the posterior territory of the left middle cerebral artery on Day 3. (**D1** and **D2**) On Day 7, a new delayed ischaemic infarct is visualized in the left anterior middle cerebral artery territory including the recording area. Moreover, a small delayed infarct is seen in the left anterior cerebral artery territory. (**E**) The initial spreading depolarization of the cluster is displayed that is completely depicted at lower resolution in Fig. 5. The cluster occurred on Day 4 after aneurismal SAH between the two MRIs of Days 3 and 7. Traces 1–5 show the near-DC/AC-electrocorticography recordings at subdural electrodes E1 to E5 measured by the GT205 amplifier whereas traces 6–10 simultaneously give the DC/AC-electrocorticography recordings measured by the BrainAmp amplifier. Note that the slow potential change is distorted in the near-DC/AC-electrocorticography recordings in traces 2–5, which precludes assessment of its duration (Hartings *et al.*, 2009) in contrast to the slow potential change depicted in the DC/AC-electrocorticography recordings in traces 7–10. The slow potential change propagates from electrode E5 to E2 (arrows). Trace 11 (blue) provides the slow potential change simultaneously measured by electrode FC5 at the scalp. Traces 12–16 depict the spreading depression of spontaneous activity in the power of the AC-electrocorticography at subdural electrodes E1 to E5. The lowest trace (green) displays the tissue partial pressure of oxygen. Abrupt, marked reduction of tissue oxygen accompanies spreading depolarization as measured close to electrode E6 using an intraparenchymal oxygen sensor (Licox, Integra Lifesciences Corporation). This may be the consequence of a combination of reduced blood supply (inverse coupling) with increased oxygen consumption in response to spreading depolarization (Dreier *et al.*, 2009). Note that the spreading depolarization does not propagate to subdural electrode E1. Electrode E1 was positioned on a neighbouring gyrus that was not affected by the new infarct. Because of artefacts in lower frequencies, we chose a bandpass between 30 and 45 Hz to illustrate the depression of spontaneous activity in the subdural recordings.

Isolated depression periods in scalp and cortical surface recordings of patients with aneurismal subarachnoid haemorrhage

In 239 of the 275 spreading depolarizations, near-DC/AC-electrocorticography displayed spreading depression of spontaneous activity. Unfortunately, in 34 of those, depression of spontaneous activity escaped detection in the AC-EEG due to an artefact produced by the automatic drift correction of the BrainAmp amplifier. The automatic drift correction had to be turned on since substantial slow drifts of the EEG signal could occur over the long recording periods. For each of the remaining 205 spreading depolarizations, we identified the AC-electrocorticography channel with the longest and the shortest depression periods using the integral of power of the cortical surface recordings (Fig. 1A). As explained previously, the depression period is an indirect indicator of tissue energy supply since restoration of the spontaneous activity after spreading depolarization is energy dependent (Back *et al.*, 1994; Dreier *et al.*, 2006). In the 205 spreading depolarizations, the median longest depression period

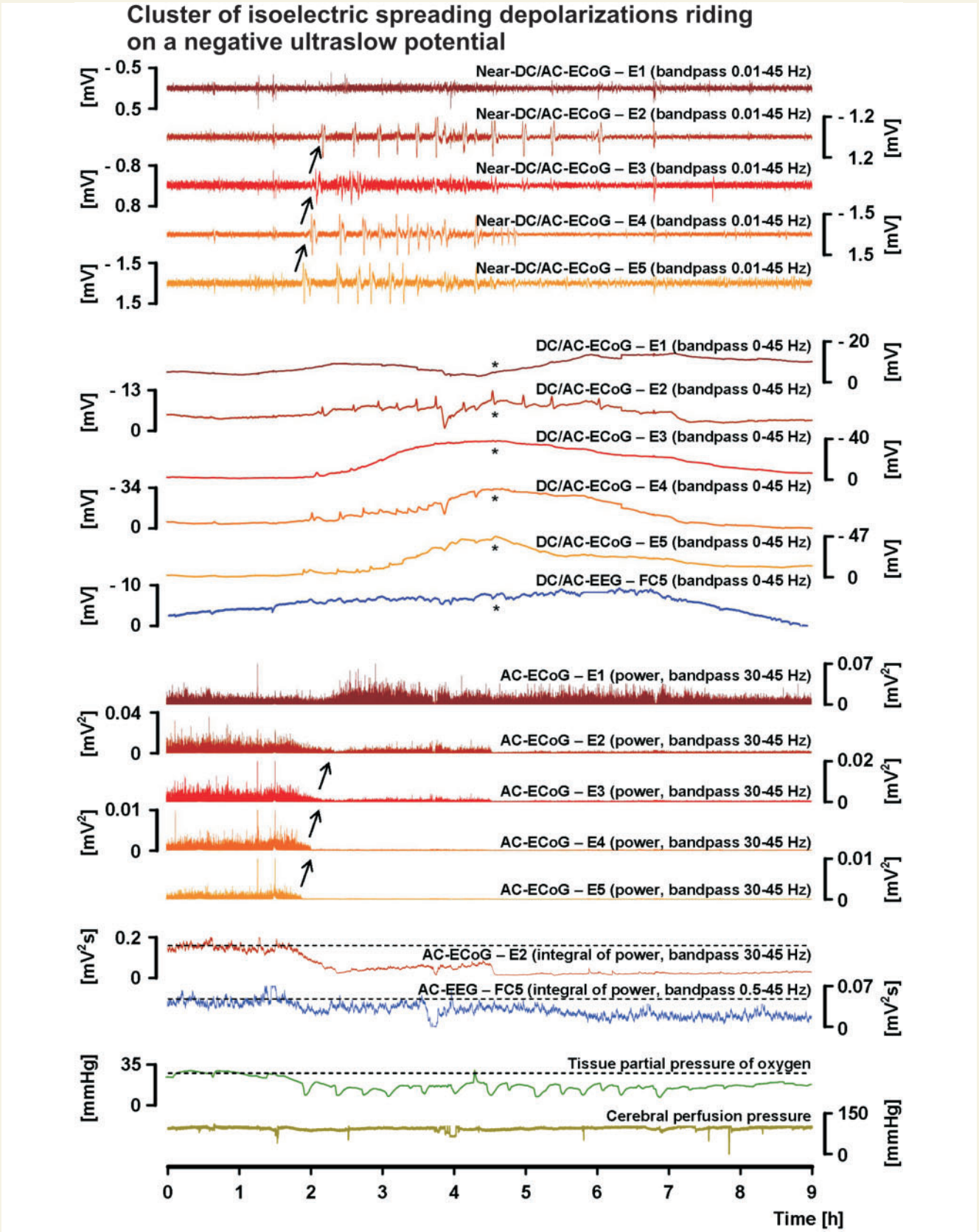

Figure 5 Cluster of silent spreading depolarizations riding on a negative ultraslow potential during development of a new delayed ischaemic infarct (Case 2 in Table 1). Figure 4 depicts the first spreading depolarization of this cluster at high resolution in addition to the neuroimaging findings. Similar to Fig. 4, traces 1–5 show the near-DC/AC-electrocorticography (ECoG) recordings at subdural electrodes E1 to E5 measured by the GT205 amplifier, whereas traces 6–10 simultaneously give the DC/AC-electrocorticography recordings

(continued)

lasted for 12.6 (9.5, 16.8) min and the median shortest depression period for 5.0 (4.1, 8.1) min. During the longest depression period, the integral of power fell to 23.6 (10.5, 35.2)%, and, during the shortest depression period, to 24.2 (14.2, 34.0)%. In only 96 of the 205 spreading depolarizations (46.8%), visual inspection of the AC-EEG identified depression of spontaneous activity. Figure 1 shows examples for such scalp EEG detected depression periods. Proportions of spreading depolarizations with AC-electrocorticography depression that also displayed AC-EEG depression of spontaneous activity ranged from 30% to 75% for the five individual patients with aneurismal SAH. During depression, the integral of scalp AC-EEG power decreased to a median value of 52.5 (36.2, 64.1)% (range: 10.8–82.1%).

Subsequently, we compared the 96 spreading depolarizations where AC-EEG displayed depression periods with the 109 spreading depolarizations where this was not the case. Of note, the interval between successive spreading depolarizations were significantly longer for spreading depolarizations during which AC-EEG displayed a depression period [44.0 (28.0, 132.0) versus 30.0 (26.5, 51.5) min, $P = 0.001$, $n = 205$, Mann–Whitney Rank Sum Test] (Table 2). Moreover, spontaneous activity was depressed to a significantly lower level [integral of AC-electrocorticography power reduction to 15.8 (7.3, 34.7) versus 27.1 (12.5, 35.6)% during the longest depression period, $P = 0.004$, $n = 205$, Mann–Whitney Rank Sum Test]. The EEG reflects a summation of volume-conducted signals from cortical generators widely distributed over the whole hemisphere. These findings thus suggest that highly frequent spreading depolarizations with depression of spontaneous activity in the AC-electrocorticography led to fusion of depression periods in the AC-EEG between subsequent spreading depolarizations. This process is illustrated in Fig. 3A and B.

We then investigated whether the durations of either shortest or longest AC-electrocorticography depression period of spontaneous activity correlated with the duration of the AC-EEG depression period. Both correlated significantly with the AC-EEG depression period ($n = 96$; shortest depression: correlation coefficient: 0.301, $P = 0.003$; longest depression: correlation coefficient: 0.233, $P = 0.023$, Spearman's Rank Order Correlation). We also studied whether the levels to which the spontaneous electrocorticography activity was depressed during the shortest and longest depression periods, respectively, correlated with the level to which the EEG was depressed. Again, significant correlations were found ($n = 96$; shortest depression: correlation coefficient: 0.287, $P = 0.005$; longest depression: correlation coefficient: 0.435, $P < 0.001$, Spearman's Rank Order Correlation). Consistent with the findings for slow potential changes at scalp electrodes, there was no observable spread of AC-EEG depression between scalp electrodes (Fig. 1A). Onset of AC-EEG depression and slow potential change could precede, accompany or succeed onset of AC-electrocorticography depression and slow potential change for different spreading depolarizations of the same patient as shown in Fig. 1B. This change in temporal relationships between brain surface near-DC/AC-electrocorticography and scalp DC/AC-EEG corresponded with different propagation paths in the near-DC/AC-electrocorticography recordings (Fig. 1B). Median delay between AC-electrocorticography and AC-EEG depressions was 5.3 (2.1, 10.1) min.

Patients with malignant hemispheric stroke

Demographic details are given in Table 1. During 475.6 h of near-DC/AC-electrocorticography recording time, the four patients with MHS had a total of 79 spreading depolarizations. For further analysis, 268.2 h of simultaneous near-DC/AC-electrocorticography and DC/AC-EEG recording time was available during which 20 of the 79 spreading depolarizations were observed. The slow potential change of these spreading depolarizations had a peak-to-peak amplitude of 4.5 (3.5, 5.2) mV in the near-DC-electrocorticography and a propagation velocity of 6.1 (3.2, 7.6) mm/min. There was only one silent, clustered spreading depolarization. Hence, 19 spreading depolarizations induced AC-electrocorticography depression of spontaneous activity. Unfortunately, 12 of these were not detected in the scalp DC/AC-EEG due to the artefact produced by the automatic DC drift correction of the BrainAmp amplifier. The remaining seven spreading depolarizations from three of the four patients showed a depression to 50.4 (34.1, 59.1)% similar to the median depression in the patients with aneurismal SAH and lasted for 10.5 (9.4, 22.6) min. The simultaneous shortest and

Figure 5 Continued
measured by the BrainAmp amplifier. The near-DC/AC- and DC/AC-electrocorticography recordings display the slow potential changes that identify the spreading depolarizations. The arrow marks the first spreading depolarization in traces 2–5. The first spreading depolarization causes persistent spreading depression of spontaneous activity, as shown in traces 13–16 (power of subdural electrodes E1–E5, arrows), trace 17 (integral of power at electrode E2) and trace 18 (integral of power at scalp electrode FC5). The multiple subsequent spreading depolarizations in traces 2–5 and 7–10, respectively, occur during this persistent depression of spontaneous activity (silent spreading depolarizations). Note in the DC/AC-electrocorticography recordings of traces 7–10 that the recurrent slow potential changes ride on a negative ultraslow potential (marked by the stars). This negative ultraslow injury potential is largest at electrodes E3 to E5 and seems reflected in a shallow negative ultraslow potential at scalp electrode FC5 (trace 11). Note that no slow potential changes/spreading depolarizations occur at subdural electrode E1 which was located on another gyrus spared from infarction. Interestingly, an ultraslow positive potential (current source) is seen at subdural electrode E1 (star at trace 6) in contrast to the ultraslow negative potential (current sink) at the other electrodes, remarkably similar to findings in and around infarcts in animals (Oliveira-Ferreira *et al.*, 2010). Trace 19 shows a persistent decrease of tissue partial pressure of oxygen as measured with an oxygen sensor. Note recurrent decreases of tissue oxygen in response to the spreading depolarizations. Cerebral perfusion pressure is constant during the event. Because of artefacts in lower frequencies, we chose a bandpass between 30 and 45 Hz to illustrate the depression of spontaneous activity in the subdural recordings.

longest AC-electrocorticography depression periods lasted for 7.7 (6.4, 15.3) and 2.8 (2.3, 3.7) min, respectively; the integral of AC-electrocorticography power was depressed to 24.7 (17.9, 34.4) and 29.7 (21.4, 49.5)%, respectively. In the scalp DC-EEG recordings, median slow potential change amplitude was −305 (range: −107, −517) μV and median slow potential change duration was 7.4 (4.4, 8.3) min. Correlations between electrocorticography and EEG parameters were not analysed because of insufficient statistical power.

Discussion

It has been known for a long time that cerebral ischaemia is associated with marked changes in the human scalp AC-EEG, such as polymorphic delta activity, focal attenuation as well as loss of fast activity and sleep spindles (Cohn *et al.*, 1948). These changes in spontaneous activity were first used diagnostically for the intraoperative monitoring during carotid endarterectomy (Sharbrough *et al.*, 1973). Later, a number of approaches using scalp AC-EEG have been developed to detect the advent of delayed cerebral ischaemia in patients with aneurismal SAH (Labar *et al.*, 1991; Rivierez *et al.*, 1991; Vespa *et al.*, 1997; Claassen *et al.*, 2004, 2005). Clinical application of quantitative AC-EEG technology was tested in different studies and was found clinically useful in the screening for delayed cerebral ischaemia. The best quantitative AC-EEG parameter for this purpose has remained controversial. Ratios of fast over slow activity and trend analysis of total power, in similar fashion to our study, are among the favoured approaches (Labar *et al.*, 1991; Vespa *et al.*, 1997; Claassen *et al.*, 2005). It is seen as a strength of scalp AC-EEG that the changes associated with delayed cerebral ischaemia are widespread so these changes provide a summary measure for very different locations of the cerebrum that can be affected by delayed cerebral ischaemia. Use at the bedside is another obvious advantage of scalp EEG. On the other hand, there are some disadvantages: artefacts by scalp electrodes may confound neuroimaging studies (Claassen *et al.*, 2005). Moreover, interpretation of quantitative AC-EEG parameters has been only recommended with caution (Claassen *et al.*, 2005). They should not be interpreted in isolation but in combination with the underlying raw AC-EEG by a person trained in this analysis since a multitude of artefacts as well as extracranial factors such as scalp swelling may confound them. Furthermore, labour intensity is a problem for continuous EEG recording, an EEG technician being constantly needed to ensure high-quality measurements and neurophysiologists having to evaluate enormous amounts of EEG data.

Classic diagnostic tools for detection of ischaemic lesion progression

Quantitative AC-EEG in isolation is not sufficient for the diagnosis of delayed cerebral ischaemia but it serves as a screening tool (Claassen *et al.*, 2005). This implies that additional studies are currently needed to confirm the diagnosis of delayed cerebral ischaemia such as clinical examination, digital subtraction angiography, transcranial Doppler sonography or neuroimaging (Claassen *et al.*, 2005). Unfortunately, these confirmatory studies have limitations as well: clinical examinations are of limited value in stuporous or comatose patients with aneurismal SAH. Digital subtraction angiography remains the gold standard for the diagnosis of proximal vasospasm but is not without risk for the patient, and the value of digital subtraction angiography for the diagnosis of delayed cerebral ischaemia has been increasingly questioned in recent years (Vergouwen *et al.*, 2010). First, there is now clear evidence from autopsy and neuroimaging studies that delayed cerebral ischaemia can occur without angiographic vasospasm (Neil-Dwyer *et al.*, 1994; Dreier *et al.*, 2002; Weidauer *et al.*, 2008; Woitzik *et al.*, 2011). Moreover, in contrast to a significant association between unfavourable clinical outcome and delayed cerebral ischaemia (Vergouwen *et al.*, 2011), in a recent meta-analysis, no association was found between unfavourable outcome and proximal vasospasm (Etminan *et al.*, 2011). The validity of transcranial Doppler-sonography for the diagnosis of delayed cerebral ischaemia is even more restricted since, as a surrogate method for digital subtraction angiography, significant correspondence between digital subtraction angiography and transcranial Doppler-sonography was only found for relatively small ranges of transcranial Doppler-sonography mean velocities in the middle cerebral arteries <120 and >200 cm/s (Vora *et al.*, 1999). CT is a reliable tool to detect delayed territorial infarcts but lesion maturation takes several hours before CT reliably identifies an infarct and so diagnosis is delayed. Moreover, cortical infarcts are the predominant pathomorphological correlate of delayed cerebral ischaemia in autopsy studies but frequently escape detection by CT (Neil-Dwyer *et al.*, 1994; Dreier *et al.*, 2002; Weidauer *et al.*, 2008). Furthermore, with few exceptions, CT is not a bedside tool but requires transport to the scanner tying up human resources from the hospital. MRI is the gold standard for the detection of delayed ischaemic stroke since its sensitivity for small lesions is significantly higher compared with that of CT (Shimoda *et al.*, 2001; Dreier *et al.*, 2002; Vergouwen *et al.*, 2010). Nevertheless, mild ischaemia without structural injury still escapes detection by MRI. Moreover, MRI shares with CT the transport problem of the patient between scanner and intensive care unit. Other methods of complementary value are imaging techniques assessing cerebral blood flow but their practical use is limited by the enormous temporal dynamics of cerebral blood flow that can drop to ischaemic levels within seconds and change to hyperperfusion within minutes up to hours thereafter as observed in a characteristic fashion using continuous subdural laser-Doppler flowmetry in patients with aneurismal SAH (Dreier *et al.*, 2009). This behaviour corresponds well with the marked diversity of cerebral blood flow patterns in imaging studies of delayed cerebral ischaemia (Minhas *et al.*, 2003).

Continuous quantitative neuromonitoring at the bedside for detection of ischaemic lesion progression

The combination of the invasive neuromonitoring tools such as subdural DC/AC-electrocorticography, tissue partial pressure of

oxygen measurements, laser-Doppler flowmetry of regional cerebral blood flow and slow and rapid sampling microdialysis now allow for the assessment of early and delayed pathophysiology in patients with aneurismal SAH and MHS in practically the same detail as in animal studies (Dreier *et al.*, 2009; Bosche *et al.*, 2010; Feuerstein *et al.*, 2010; Oliveira-Ferreira *et al.*, 2010). Cut-off values for these methods are currently being developed to guide treatment allocation in patients at risk for delayed cerebral ischaemia (Dreier, 2011). However, such cut-off values could be limited by the more or less restricted sample volumes of the invasive tools. The largest sample volume may be that of DC/AC-electrocorticography since spreading depolarizations invade the tissue surrounding the ischaemic zone and high recurrence rates may indicate even remotely developing ischaemic lesions (Dreier *et al.*, 2006; Dohmen *et al.*, 2008; Oliveira-Ferreira *et al.*, 2010). However, even if reliable cut-off values are calculated for early diagnosis of delayed cerebral ischaemia after aneurismal SAH or ischaemic lesion progression after MHS, a slight risk for local infection or haemorrhage will remain with invasive probes (Espinosa *et al.*, 1994; Lee *et al.*, 2000). This obstacle will limit probe implantation to patients requiring neurosurgical interventions. Therefore, the ultimate goal for diagnostic development is powerful, non-invasive recording technology for use at the bedside that has been validated by comparison with invasive technology. The present study represents a significant first step in this process as our invasive near-DC- and DC/AC-electrocorticography recordings have demonstrated the pathophysiological basis of the previously described scalp AC-EEG changes in the course of aneurismal SAH and ischaemic stroke. Our findings thus indicate that the characteristic loss of AC-EEG power associated with ischaemia (Labar *et al.*, 1991; Vespa *et al.*, 1997; Claassen *et al.*, 2004) is caused by clusters of spreading depolarizations associated with the depression of spontaneous activity.

In addition, we have identified two other, promising signals while recording the DC-component of the scalp EEG. It was not believed possible to record the slow potential change, the extracellular index of spreading depolarization, in scalp DC-EEG recordings as the potent capacitive resistance of dura and skull would filter the slow voltage variation (Dreier, 2011). In the present study, the large majority of slow potential changes in the near-DC- and DC-electrocorticography were nevertheless accompanied by slow potential changes in the scalp DC-EEG. Furthermore, in two cases, scalp DC-EEG recordings were performed during early infarct evolution, and scalp electrodes were placed over the infarcting area. In these cases, scalp DC-EEG recorded a negative ultraslow potential, the classical extracellular index of neuronal injury in animal experiments (Herreras and Somjen, 1993; Lehmenkühler *et al.*, 1999; Oliveira-Ferreira *et al.*, 2010). In one of these cases, DC-electrocorticography was recorded at the cortical surface in addition to the routine near-DC-electrocorticography while the subdural electrode strip overlaid the region of the developing infarct. This allowed us to measure in parallel the negative ultraslow injury potential at both scalp and cortical surface. Similar to recordings in rats, the DC-shifts of spreading depolarizations did not reverse between cortical surface and scalp as these potentials are generated in the parenchyma rather than at the interface between blood and brain (Lehmenkühler *et al.*, 1991). However, future experimental studies should address whether and how the signals are influenced by the fresh craniotomy in the patients with aneurismal SAH or by the decompressive hemicraniectomy in the patients with MHS.

Visual inspection did not detect a spread of slow potential change or AC-EEG depression of spontaneous activity between different scalp electrodes. This is likely explained by the fact that the scalp EEG is influenced by volume conduction from many superposed sources of the whole hemisphere. For spread reconstruction, disentanglement of cortical generators from scalp DC/AC-EEG recordings would require more complex mathematical procedures such as virtual source montage or principal components analysis (Miller *et al.*, 2007).

Conclusion and future goals

The strength of the combined bedside recording of the scalp ultraslow potential, slow potential change and depression of spontaneous activity is that they potentially allow for the instantaneous, on-line detection of ischaemic injury onset and progression in a large patient population. This would allow for targeted treatment to begin earlier than with diagnosis based on any imaging modality, which requires time for lesion maturation as well as time for patient transport to the scanner. To come to this point, the electrophysiological techniques require further development and careful analysis of limitations. In principle, the negative ultraslow potential of ischaemic injury is the largest electrophysiological signal at the human brain surface (Leão, 1947; Oliveira-Ferreira *et al.*, 2010), even larger than the slow potential change, which can reach up to 25 mV (Dreier *et al.*, 2009; Oliveira-Ferreira *et al.*, 2010) and much larger than the DC potential associated with epileptic seizure activity, which may reach up to 2 mV at the cortical surface (Dreier *et al.*, 2012) and 30–150 μV at the scalp (Miller *et al.*, 2007). However, the DC potential can be confounded by many different generators including the eyeball, tongue, blood–brain barrier and the skin (Miller *et al.*, 2007). The galvanic skin response at the scalp can be avoided by slight puncturing of the skin epithelia during electrode application. Other causes of DC potentials such as movements, jugular vein compression or chemical factors like changes in carbon dioxide tension, are more difficult to control, and not all DC potential generators may be known.

Further development of the techniques applied here could make it possible in the future to alert the neurointensive care specialist of the onset or progression of neuronal injury in a fashion similar to the use of continuous electrocardiography to detect cardiac arrhythmia. A number of research goals have to be achieved for this purpose. Thus, it is necessary to calculate sensitivity and specificity for a cut-off value of duration in spreading depolarization-induced depression of spontaneous activity measured by electrocorticography or EEG that indicates delayed ischaemic stroke after aneurismal SAH or ischaemic lesion progression in MHS, lesion progression being assessed using serial MRI (Dreier, 2011). For this analysis, recording of slow potential changes would serve the differentiation between spreading depolarization-induced depression and other types of depression

such as depression of spontaneous activity by sedatives for example. Moreover, a better understanding of the complex generators and artefacts underlying DC potential changes at the brain surface and scalp is needed to make full use of slow potential change and ultraslow potential. Polymer researchers should develop electrodes with similar low-frequency recording properties as Ag/AgCl electrodes but without their toxicity to replace the platinum electrodes for the subdural recordings. Platinum has much better low-frequency recording properties than stainless steel but is polarizable and thus inferior to Ag/AgCl (Tallgren *et al.*, 2005). Mathematical tools such as virtual source montage and principal components analysis should be applied to identify the characteristic propagation of spreading depolarizations using scalp DC/AC-EEG in analogous fashion to the source localization of epileptic seizure activity (Miller *et al.*, 2007). The spread would add another criterion to distinguish spreading depolarizations from other bioelectrical phenomena and artefacts. Electrocorticography recordings at the brain surface could be used to validate such mathematical tools since they identify with high accuracy sources of slow potential changes. Additional criteria for the differential diagnosis of electrophysiological signals could be derived from non-invasive surrogate measures of cerebral blood flow such as near-infrared or diffuse correlation spectroscopy that can be applied at the bedside (Obrig and Villringer, 2003; Durduran *et al.*, 2010). All this should be flanked by the development of software packages and hardware for automated, on-line analysis at the bedside on the intensive care unit. We believe that the findings of the present study are promising for this development since, in all patients, even visual inspection of the raw time-compressed DC/AC-EEG data was sufficient to identify clear reflections of the spreading depolarizations at the scalp.

Acknowledgements

We would like to thank the nursing staff of the study, Claudia Altendorf and Nicole Gase.

Funding

Deutsche Forschungsgemeinschaft (DFG) DFG DR 323/5-1 to J.P.D. and J.W., DFG SFB Tr3 D10; Bundesministerium für Bildung und Forschung (Center for Stroke Research Berlin, 01 EO 0801 and Bernstein Center for Computational Neuroscience Berlin 01GQ1001C B2); ERA-NET NEURON SDSVD German Israeli Foundation (No 124/2008); Wilhelm Sander foundation (2002.028.1); Kompetenznetz Schlaganfall to J.P.D. and DFG WO 1704/1-1 to J.W. M.S. was supported by the 'Friedrich C. Luft' Clinical Scientist Pilot Program funded by Volkswagen Foundation and Charité Foundation.

References

Back T, Kohno K, Hossmann KA. Cortical negative DC deflections following middle cerebral artery occlusion and KCl-induced spreading depression: effect on blood flow, tissue oxygenation, and electroencephalogram. J Cereb Blood Flow Metab 1994; 14: 12–9.

Bosche B, Graf R, Ernestus RI, Dohmen C, Reithmeier T, Brinker G, et al. Recurrent spreading depolarizations after SAH decrease oxygen availability in human cerebral cortex. Ann Neurol 2010; 67: 607–17.

Canals S, Makarova I, Lopez-Aguado L, Largo C, Ibarz JM, Herreras O. Longitudinal depolarization gradients along the somatodendritic axis of CA1 pyramidal cells: a novel feature of spreading depression. J Neurophysiol 2005; 94: 943–51.

Claassen J, Hirsch LJ, Kreiter KT, Du EY, Connolly ES, Emerson RG, et al. Quantitative continuous EEG for detecting delayed cerebral ischemia in patients with poor-grade subarachnoid hemorrhage. Clin Neurophysiol 2004; 115: 2699–710.

Claassen J, Mayer SA, Hirsch LJ. Continuous EEG monitoring in patients with subarachnoid hemorrhage. J Clin Neurophysiol 2005; 22: 92–8.

Cohn R, Raines GN, Mulder DW, Neumann MA. Cerebral vascular lesions; electroencephalographic and neuropathologic correlations. Arch Neurol Psychiatry 1948; 60: 165–81.

Dohmen C, Sakowitz OW, Fabricius M, Bosche B, Reithmeier T, Ernestus RI, et al. Spreading depolarizations occur in human ischemic stroke with high incidence. Ann Neurol 2008; 63: 720–8.

Donnan GA. The 2007 Feinberg lecture: a new road map for neuroprotection. Stroke 2008; 39: 242.

Dreier JP. The role of spreading depression, spreading depolarization and spreading ischemia in neurological disease. Nat Med 2011; 17: 439–47.

Dreier JP, Major S, Manning A, Woitzik J, Drenckhahn C, Steinbrink J, et al. Cortical spreading ischaemia is a novel process involved in ischaemic damage in patients with aneurysmal subarachnoid haemorrhage. Brain 2009; 132: 1866–81.

Dreier JP, Major S, Pannek HW, Woitzik J, Scheel M, Wiesenthal D, et al. Spreading convulsions, spreading depolarization, and epileptogenesis in human cerebral cortex. Brain 2012; 135: 259–76.

Dreier JP, Sakowitz OW, Harder A, Zimmer C, Dirnagl U, Valdueza JM, et al. Focal laminar cortical MR signal abnormalities after subarachnoid hemorrhage. Ann Neurol 2002; 52: 825–9.

Dreier JP, Woitzik J, Fabricius M, Bhatia R, Major S, Drenckhahn C, et al. Delayed ischaemic neurological deficits after subarachnoid haemorrhage are associated with clusters of spreading depolarizations. Brain 2006; 129: 3224–37.

Durduran T, Choe R, Baker WB, Yodh AG. Diffuse optics for tissue monitoring and tomography. Rep Progr Phys 2010; 73: 076701.

Espinosa J, Olivier A, Andermann F, Quesney F, Dubeau F, Savard G. Morbidity of chronic recording with intracranial depth electrodes in 170 patients. Stereotact Funct Neurosurg 1994; 63: 63–5.

Etminan N, Vergouwen MD, Ilodigwe D, Macdonald RL. Effect of pharmaceutical treatment on vasospasm, delayed cerebral ischemia, and clinical outcome in patients with aneurysmal subarachnoid hemorrhage: a systematic review and meta-analysis. J Cereb Blood Flow Metab 2011; 31: 1443–51.

Fabricius M, Fuhr S, Bhatia R, Boutelle M, Hashemi P, Strong AJ, et al. Cortical spreading depression and peri-infarct depolarization in acutely injured human cerebral cortex. Brain 2006; 129: 778–90.

Fabricius M, Fuhr S, Willumsen L, Dreier JP, Bhatia R, Boutelle MG, et al. Association of seizures with cortical spreading depression and peri-infarct depolarisations in the acutely injured human brain. Clin Neurophysiol 2008; 119: 1973–84.

Feuerstein D, Manning A, Hashemi P, Bhatia R, Fabricius M, Tolias C, et al. Dynamic metabolic response to multiple spreading depolarizations in patients with acute brain injury: an online microdialysis study. J Cereb Blood Flow Metab 2010; 30: 1343–55.

Hartings JA, Bullock MR, Okonkwo DO, Murray LS, Murray GD, Fabricius M, et al. Spreading depolarisations and outcome after traumatic brain injury: a prospective observational study. Lancet Neurol 2011a; 10: 1058–64.

Hartings JA, Strong AJ, Fabricius M, Manning A, Bhatia R, Dreier JP, et al. Spreading depolarizations and late secondary insults after traumatic brain injury. J Neurotrauma 2009; 26: 1857–66.

Hartings JA, Watanabe T, Dreier JP, Major S, Vendelbo L, Fabricius M. Recovery of slow potentials in AC-coupled electrocorticography: application to spreading depolarizations in rat and human cerebral cortex. J Neurophysiol 2009; 102: 2563–75.

Hartings JA, Watanabe T, Bullock MR, Okonkwo DO, Fabricius M, Woitzik J, et al. Spreading depolarizations have prolonged direct current shifts and are associated with poor outcome in brain trauma. Brain 2011b; 134: 1529–40.

Herreras O, Somjen GG. Analysis of potential shifts associated with recurrent spreading depression and prolonged unstable spreading depression induced by microdialysis of elevated K+ in hippocampus of anesthetized rats. Brain Res 1993; 610: 283–94.

Hossmann KA. Viability thresholds and the penumbra of focal ischemia. Ann Neurol 1994; 36: 557–65.

Juttler E, Bosel J, Amiri H, Schiller P, Limprecht R, Hacke W, et al. DESTINY II: DEcompressive Surgery for the Treatment of malignant INfarction of the middle cerebral arterY II. Int J Stroke 2011; 6: 79–86.

Kistler JP, Crowell RM, Davis KR, Heros R, Ojemann RG, Zervas T, et al. The relation of cerebral vasospasm to the extent and location of subarachnoid blood visualized by CT scan: a prospective study. Neurology 1983; 33: 424–36.

Klatzo I. Pathophysiological aspects of brain edema. Acta Neuropathol 1987; 72: 236–9.

Klem GH, Luders HO, Jasper HH, Elger C. The ten-twenty electrode system of the International Federation. The International Federation of Clinical Neurophysiology. Electroencephalogr Clin Neurophysiol Suppl 1999; 52: 3–6.

Labar DR, Fisch BJ, Pedley TA, Fink ME, Solomon RA. Quantitative EEG monitoring for patients with subarachnoid hemorrhage. Electroencephalogr Clin Neurophysiol 1991; 78: 325–32.

LaManna JC, Rosenthal M. Effect of ouabain and phenobarbital on oxidative metabolic activity associated with spreading cortical depression in cats. Brain Res 1975; 88: 145–9.

Leão AAP. Further observations on the spreading depression of activity in the cerebral cortex. J Neurophysiol 1947; 10: 409–14.

Lee WS, Lee JK, Lee SA, Kang JK, Ko TS. Complications and results of subdural grid electrode implantation in epilepsy surgery. Surg Neurol 2000; 54: 346–51.

Lehmenkühler A, Richter F, Poppelmann T. Hypoxia- and hypercapnia-induced DC potential shifts in rat at the scalp and the skull are opposite in polarity to those at the cerebral cortex. Neurosci Lett 1999; 270: 67–70.

Lehmenkühler A, Richter F, Scheller D, Speckmann EJ. Non-invasive DC recordings from the skull and the skin during cortical spreading depression: a model of detection of migraine. In: Olesen J, editor. Frontiers in headache research Migraine and other headaches: The vascular mechanisms. New York: Raven Press; 1991. p. 167–70.

Lo EH. A new penumbra: transitioning from injury into repair after stroke. Nat Med 2008; 14: 497–500.

Miller JW, Kim W, Holmes MD, Vanhatalo S. Ictal localization by source analysis of infraslow activity in DC-coupled scalp EEG recordings. Neuroimage 2007; 35: 583–97.

Minhas PS, Menon DK, Smielewski P, Czosnyka M, Kirkpatrick PJ, Clark JC, et al. Positron emission tomographic cerebral perfusion disturbances and transcranial Doppler findings among patients with neurological deterioration after subarachnoid hemorrhage. Neurosurgery 2003; 52: 1017–22 discussion 22–4.

Nakamura H, Strong AJ, Dohmen C, Sakowitz OW, Vollmar S, Sue M, et al. Spreading depolarizations cycle around and enlarge focal ischaemic brain lesions. Brain 2010; 133: 1994–2006.

Neil-Dwyer G, Lang DA, Doshi B, Gerber CJ, Smith PW. Delayed cerebral ischaemia: the pathological substrate. Acta Neurochir (Wien) 1994; 131: 137–45.

Obrig H, Villringer A. Beyond the visible–imaging the human brain with light. J Cereb Blood Flow Metab 2003; 23: 1–18.

Oliveira-Ferreira AI, Milakara D, Alam M, Jorks D, Major S, Hartings JA, et al. Experimental and preliminary clinical evidence of an ischemic zone with prolonged negative DC shifts surrounded by a normally perfused tissue belt with persistent electrocorticographic depression. J Cereb Blood Flow Metab 2010; 30: 1504–19.

Oliveira-Ferreira AI, Winkler MKL, Reiffurth C, Milakara D, Woitzik J, Dreier JP. Spreading depolarization, a pathophysiological mechanism of stroke and migraine aura. Future Neurol 2012; 7: 45–64.

Risher WC, Ard D, Yuan J, Kirov SA. Recurrent spontaneous spreading depolarizations facilitate acute dendritic injury in the ischemic penumbra. J Neurosci 2010; 30: 9859–68.

Rivierez M, Landau-Ferey J, Grob R, Grosskopf D, Philippon J. Value of electroencephalogram in prediction and diagnosis of vasospasm after intracranial aneurysm rupture. Acta Neurochir (Wien) 1991; 110: 17–23.

Sharbrough FW, Messick JM Jr, Sundt TM Jr. Correlation of continuous electroencephalograms with cerebral blood flow measurements during carotid endarterectomy. Stroke 1973; 4: 674–83.

Shimoda M, Takeuchi M, Tominaga J, Oda S, Kumasaka A, Tsugane R. Asymptomatic versus symptomatic infarcts from vasospasm in patients with subarachnoid hemorrhage: serial magnetic resonance imaging. Neurosurgery 2001; 49: 1341–8 discussion 8–50.

Somjen GG. Mechanisms of spreading depression and hypoxic spreading depression-like depolarization. Physiol Rev 2001; 81: 1065–96.

Strong AJ, Fabricius M, Boutelle MG, Hibbins SJ, Hopwood SE, Jones R, et al. Spreading and synchronous depressions of cortical activity in acutely injured human brain. Stroke 2002; 33: 2738–43.

Takano T, Tian GF, Peng W, Lou N, Lovatt D, Hansen AJ, et al. Cortical spreading depression causes and coincides with tissue hypoxia. Nat Neurosci 2007; 10: 754–62.

Tallgren P, Vanhatalo S, Kaila K, Voipio J. Evaluation of commercially available electrodes and gels for recording of slow EEG potentials. Clin Neurophysiol 2005; 116: 799–806.

van Gijn J, Rinkel GJ. Subarachnoid haemorrhage: diagnosis, causes and management. Brain 2001; 124: 249–78.

Vergouwen MD, Etminan N, Ilodigwe D, Macdonald RL. Lower incidence of cerebral infarction correlates with improved functional outcome after aneurysmal subarachnoid hemorrhage. J Cereb Blood Flow Metab 2011; 31: 1545–53.

Vergouwen MD, Vermeulen M, van Gijn J, Rinkel GJ, Wijdicks EF, Muizelaar JP, et al. Definition of delayed cerebral ischemia after aneurysmal subarachnoid hemorrhage as an outcome event in clinical trials and observational studies: proposal of a multidisciplinary research group. Stroke 2010; 41: 2391–5.

Vespa PM, Nuwer MR, Juhasz C, Alexander M, Nenov V, Martin N, et al. Early detection of vasospasm after acute subarachnoid hemorrhage using continuous EEG ICU monitoring. Electroencephalogr Clin Neurophysiol 1997; 103: 607–15.

Vora YY, Suarez-Almazor M, Steinke DE, Martin ML, Findlay JM. Role of transcranial Doppler monitoring in the diagnosis of cerebral vasospasm after subarachnoid hemorrhage. Neurosurgery 1999; 44: 1237–47 discussion 47–8.

Wadman WJ, Juta AJ, Kamphuis W, Somjen GG. Current source density of sustained potential shifts associated with electrographic seizures and with spreading depression in rat hippocampus. Brain Res 1992; 570: 85–91.

Weidauer S, Vatter H, Beck J, Raabe A, Lanfermann H, Seifert V, et al. Focal laminar cortical infarcts following aneurysmal subarachnoid haemorrhage. Neuroradiology 2008; 50: 1–8.

Woitzik J, Dreier JP, Hecht N, Fiss I, Sandow N, Major S, et al. Delayed cerebral ischemia and spreading depolarization in absence of angiographic vasospasm after subarachnoid hemorrhage. J Cereb Blood Flow Metab 2011. Advance Access published on December 7, 2011, doi:10.1038/jcbfm.2011.169.1.